5.4 ACS SASSI FE Model of the PS/B

5.4.1 Description of the PS/B ACS SASSI Model

The PS/B ACS SASSI model is a 3-D FE model created to be transferred to ACS SASSI. The mesh size of this model is approximately 8 ft as compared to the 3 ft size of the detailed static model it is compared with for validation. The model includes shell elements representing the walls and slabs, beam elements representing beams and columns, and solid elements representing the basemat.

The stress level of the shear walls is taken under service load conditions. For those shear walls whose stress levels, including in-plane and out-of-plane stresses, are lower than the cracking stress (capacity) of the concrete, the gross section properties at the centerline are used in the model and are adjusted for openings if applicable. The material (elastic modulus) and geometric (thickness) properties of the slabs and shear walls whose in-plane shear stresses are less that concrete shear capacity but out-of-plane bending stresses are greater than concrete modulus of rupture are changed to reflect the dynamic mass and cracked concrete properties, with unchanged shear and axial stiffness and unchanged mass. The cracked concrete properties are modeled for one-half of the flexural stiffness.

Figures 5.4.1-1 through 5.4.1-6 show the ACS SASSI model at several elevations.

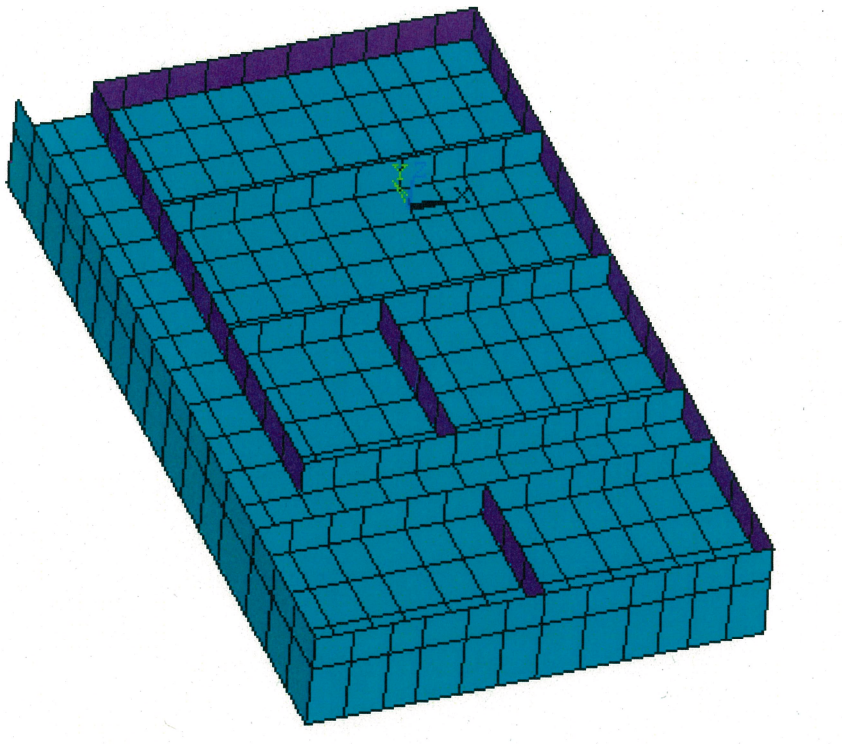

Figure 5.4.1-1 ANSYS Dynamic Model Basemat (Elev. -26'-4")

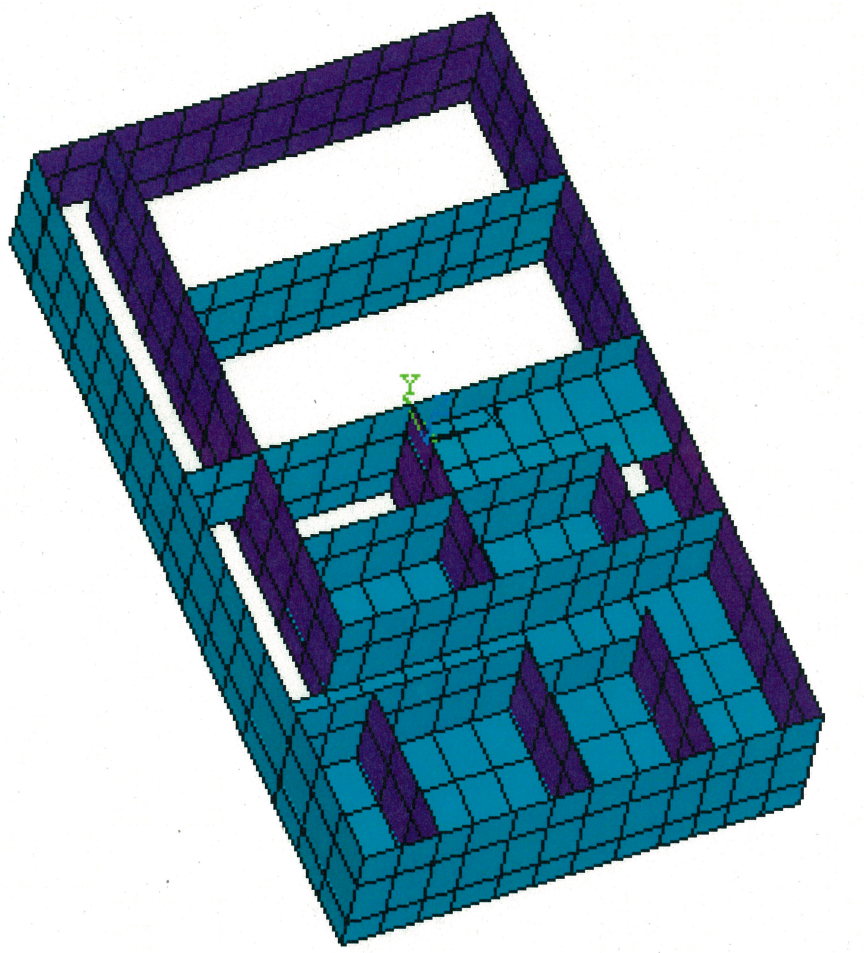

Figure 5.4.1-2 ANSYS Dynamic Model Intermediate Floor (Elev. -14’-2” & -4’-10”)

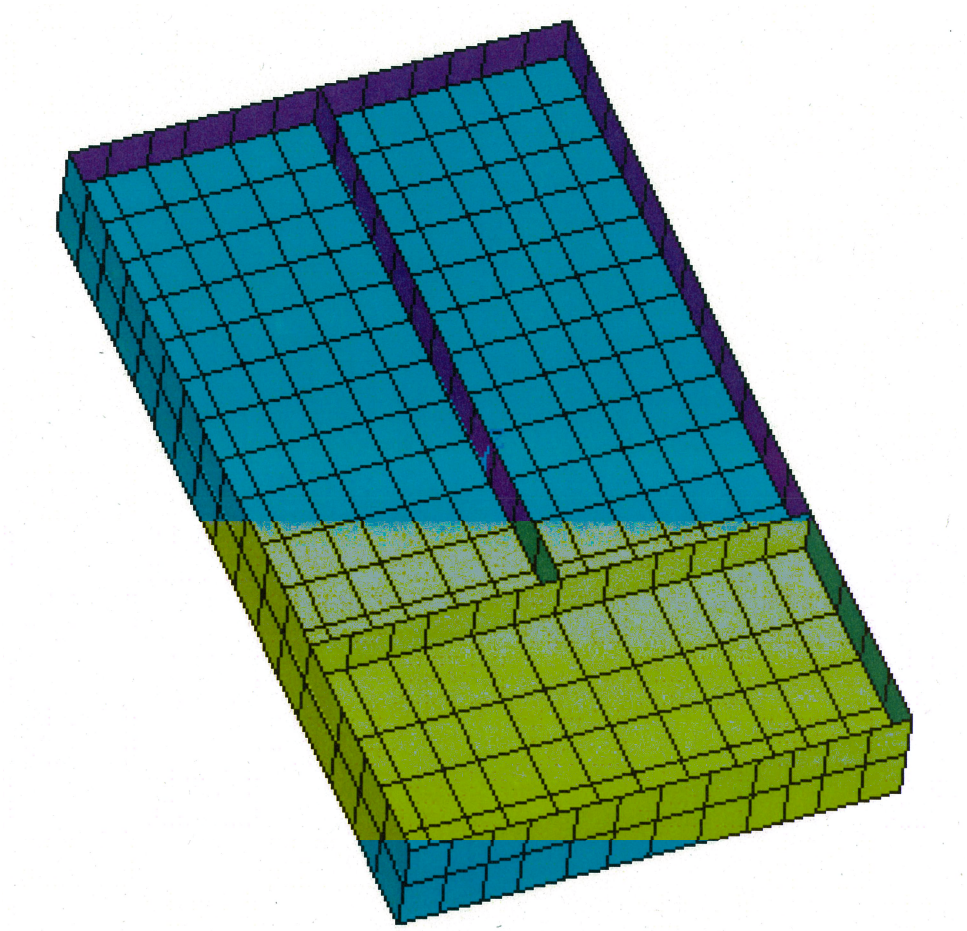

Figure 5.4.1-3 ANSYS Dynamic Model First Floor (Elev. 3'-7")

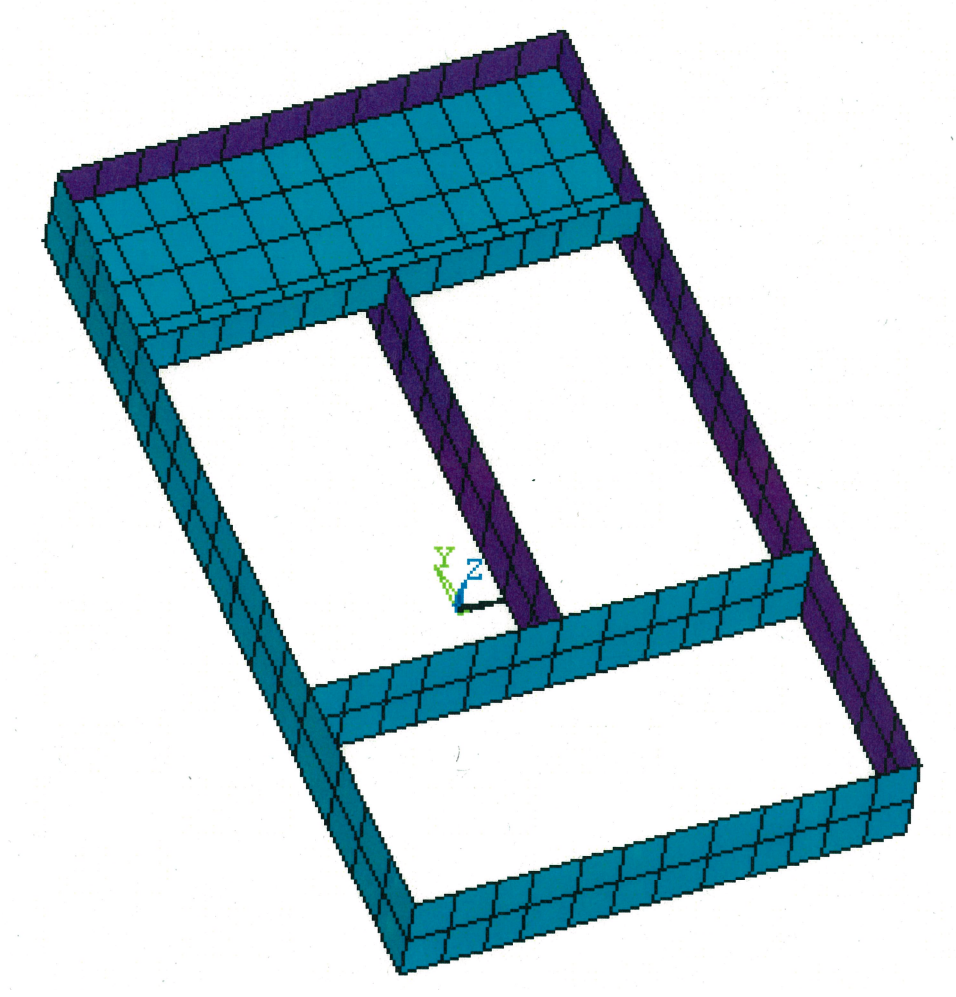

Figure 5.4.1-4 ANSYS Dynamic Model Intermediate Floor (Elev. 24'-2")

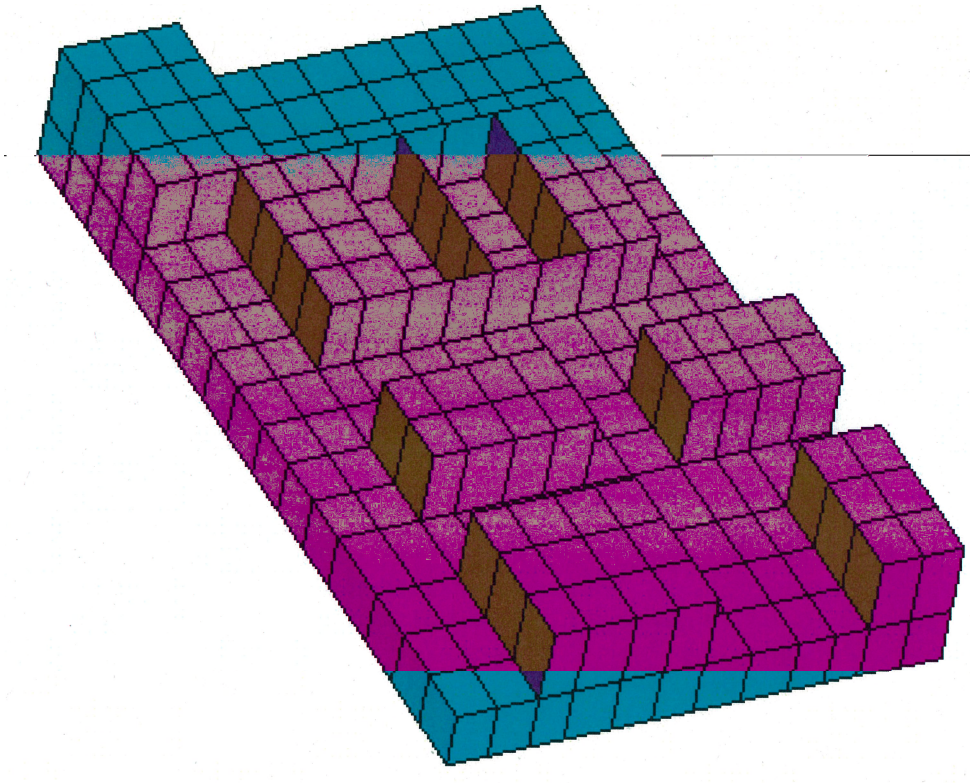

Figure 5.4.1-5 ANSYS Dynamic Model Roof (Elev. 39''-6")

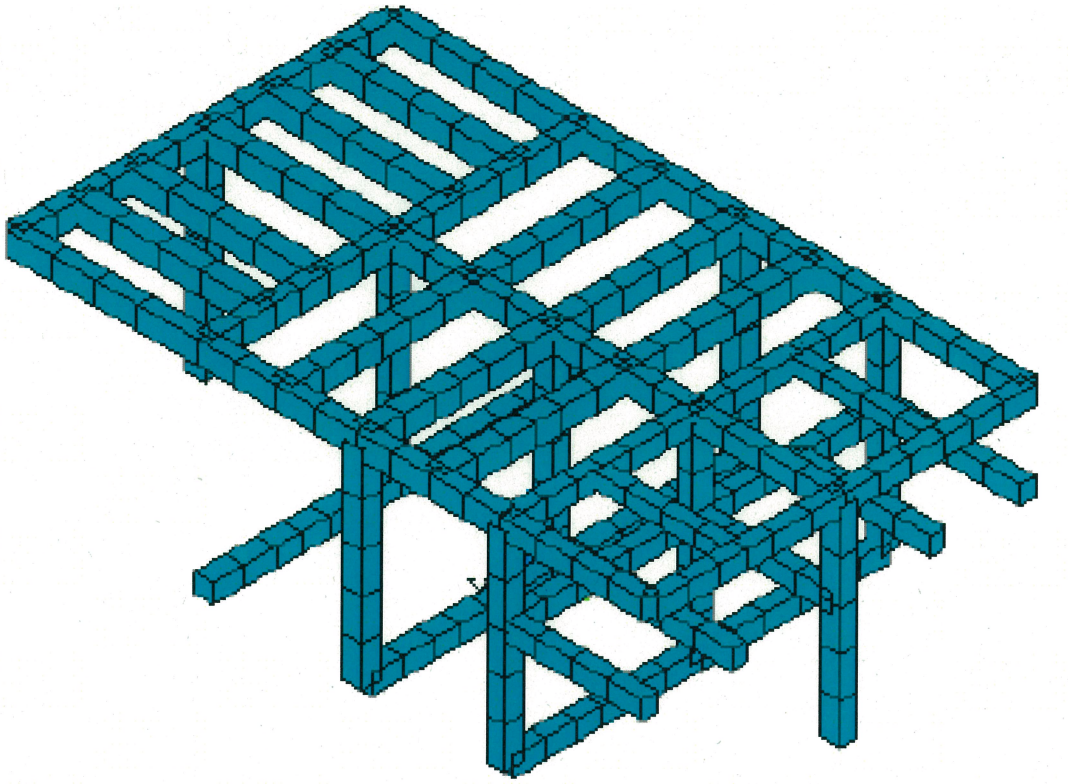

Figure 5.4.1-6 ANSYS Dynamic Model Beams & Columns

5.4.2 Validation of the PS/B ACS SASSI Model

The validation of the PS/B dynamic FE model utilizes uncracked concrete material properties. See Section 5.5 for discussion of the effects of concrete cracking.

The 1g static analysis of the ANSYS model produces several results that are compared to the 1g static analysis for validation. This includes the structural weight of the model, the mass properties, and the stiffness of the structure.

Table 5.4.2-1 presents the structural weight of the ANSYS model compared to the detailed static model. The structural weight of the DCD lumped mass stick model is also shown for comparison purposes.

Table 5.4.2-2 presents the mass properties of the ANSYS model compared to the detailed static model. These properties include the center of mass and mass inertia. The comparison shows that the center of mass and mass inertias of the two models are comparable.

Table 5.4.2-1 Structural Weight of PS/B ANSYS Model

Location	Weight (kips)			(2)/(3) ratio
	(1)	(2)	(3)	
	DCD Stick Model	ANSYS Model	Detailed Static Model	
Roof level	7890	7521[(a)]	7273[(a)]	103%
Ground Floor Level	11400	11741	11576	101%
Base Mat Level	15000	16078[(b)]	15461[(b)]	104%
Total	34290	35340	34310	103%

Notes

(a) 75% of 50 psf snow load is applied in ANSYS model, which results additional load of 275 kips comparing to the detailed static model.

(b) The detailed static model calculates the basemat weight based on the volume between center lines of the exterior walls. A weight of about (2'+8") x (111'+66') x 119" x 0.15 kcf =702 kips is not counted in the model.

Table 5.4.2-2 Mass Properties of PS/B ANSYS Model

Model	Mass Center Coordinates[(a)] (ft)			Mass Inertia about Center of Mass (kip-ft^2)		
	Xc	Yc	Zc	IXX	IYY	IZZ
(1) ANSYS Model	0.22	-1.42	-5.06	6.63E+07	4.02E+07	5.74E+07
(2) Detailed Static Model	0.37	-1.63	-4.80	6.45E+07	3.88E+07	5.65E+07
Ratio (1)/(2)				103%	104%	102%

Note

(a) Origin at geometry center of the building footprint and elevation 0'-0".

The stiffness of the structure is compared in all three directions (X, Y, and Z) using the displacement of the northwest corner of the building. Figures 5.4.2-1 through 5.4.2-3 show the displacement distributions for all three directions, respectively.

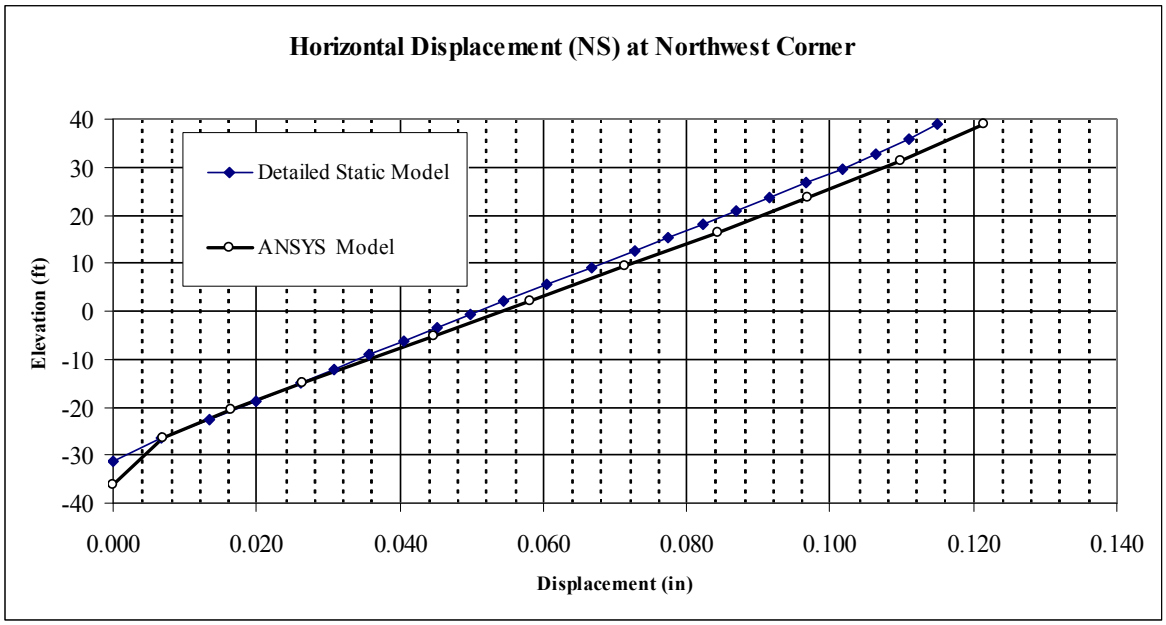

Figure 5.4.2-1 Horizontal Displacement Results Under 1g Load in NS Direction (X)

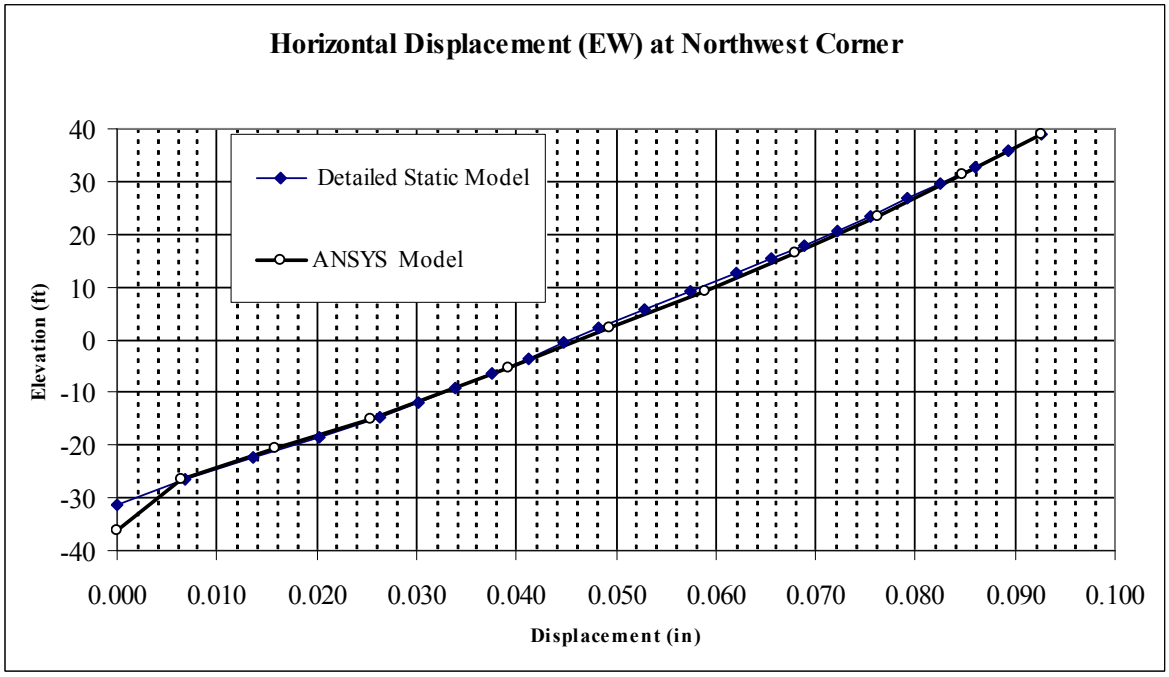

Figure 5.4.2-2 Horizontal Displacement Results Under 1g Load in EW Direction (Y)

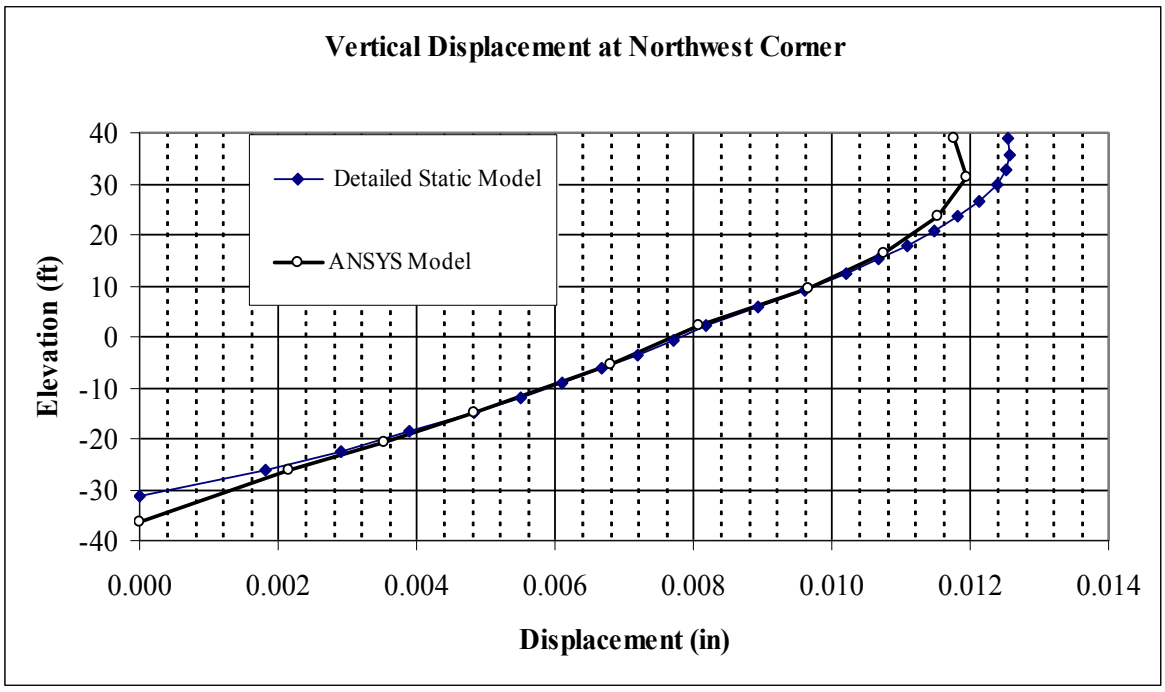

Figure 5.4.2-3 Vertical Displacement Results Under 1g Load in Vertical Direction (Z)

Several modal analyses were performed on the ANSYS model with varying mesh sizes. The comparison of the results of each analysis verifies that mesh size chosen is adequate to capture the dynamic properties of the structure. Figures 5.4.2-4 through 5.4.2-6 show the results of modal analyses for three different mesh sizes in all three directions. This includes a 3' to 5' mesh, a 5' to 8' mesh, and an 8' to 10' mesh.

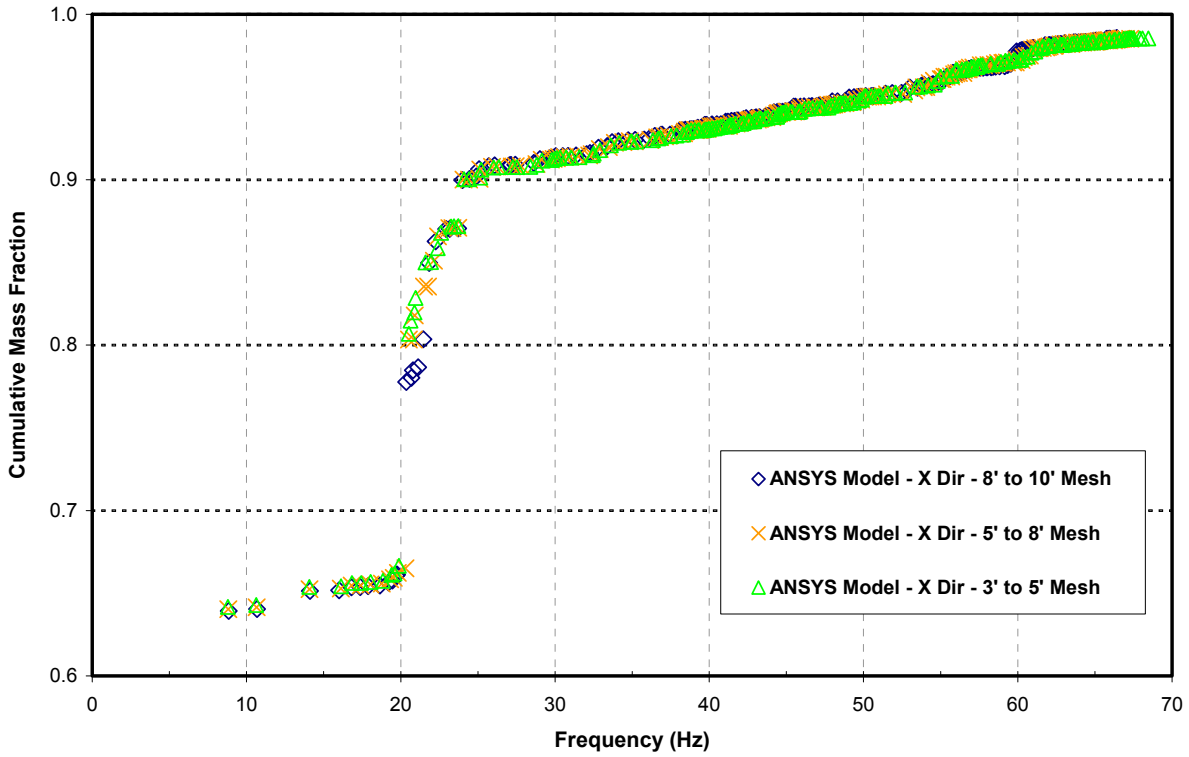

Figure 5.4.2-4 Verification of Mesh Size in X-Direction

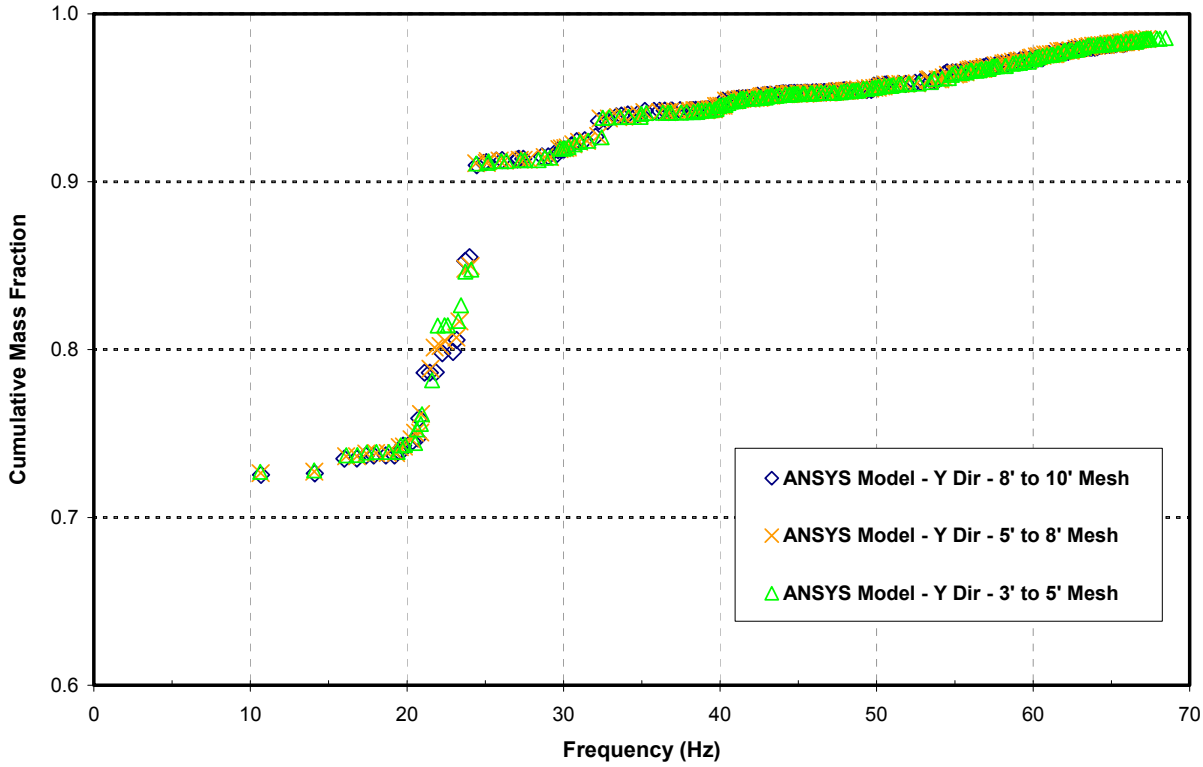

Figure 5.4.2-5 Verification of Mesh Size in Y-Direction

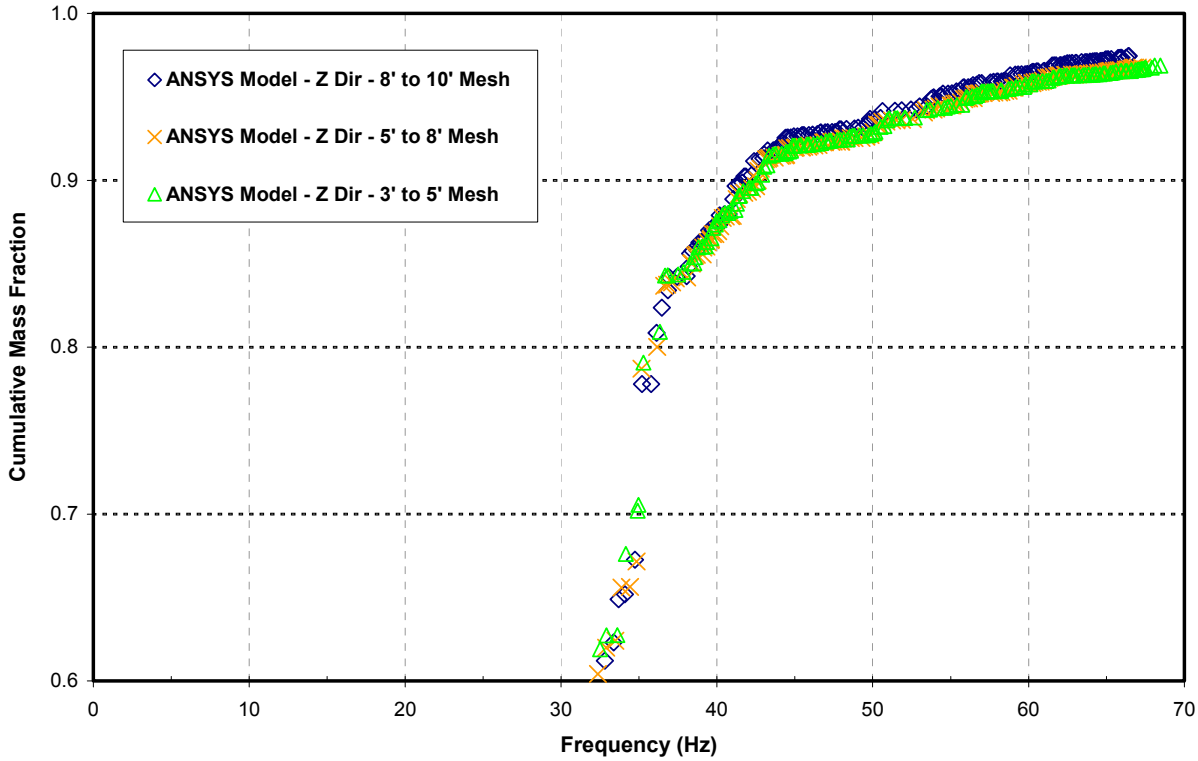

Figure 5.4.2-6 Verification of Mesh Size in Z-Direction

The ANSYS model is translated into a SASSI model using the built in converter in ACS SASSI. Validation SSI analyses are performed with the PS/B dynamic model resting on the surface of a half-space with hard-rock properties. This is to simulate the response of the structure under a fixed base condition. TFs and ARS obtained from the SASSI validation analyses at selected nodes are presented below. Modal analysis on ANSYS model with fixed base condition and uncracked concrete section properties is performed and the first 3 dominant modal properties for X, Y and Z direction vibrations are shown on Tables 5.4.2-3 thru 5.4.2-5, respectively. Those dominant modal frequencies are selected as calculation frequency steps (points) in the SSI analysis on the translated model. Transfer functions at selected representative nodes obtained from such SSI analysis are shown in Figures 5.4.2-7 thru 5.4.2-9. Those figures indicate amplification spikes at or close to the dominant frequency points and therefore validate the model translation.

Table 5.4.2-3 Modal Properties of First 3 Modes, X-Direction (N-S)

MODE	FREQUENCY (HZ)	PERIOD (sec)	PARTIC.FACTOR	EFFECTIVE MASS (Kips*sec^2/ft)
1	8.84	0.1130	21.02	441.86
13	20.36	0.0491	8.96	80.43
18	21.84	0.0458	-5.65	31.93

Table 5.4.2-4 Modal Properties of First 3 Modes, Y-Direction (E-W)

MODE	FREQUENCY (HZ)	PERIOD (sec)	PARTIC.FACTOR	EFFECTIVE MASS (Kips*sec^2/ft)
2	10.68	0.0936	22.33	498.66
24	24.45	0.0409	-6.14	37.74
22	23.72	0.0422	-5.69	32.45

Table 5.4.2-5 Modal Properties of First 3 Modes, Z-Direction (Vertical)

MODE	FREQUENCY (HZ)	PERIOD (sec)	PARTIC.FACTOR	EFFECTIVE MASS (Kips*sec^2/ft)
10	19.46	0.0514	8.2072	67.36
6	17.37	0.0576	7.5271	56.66
14	20.69	0.0483	-6.8528	46.96

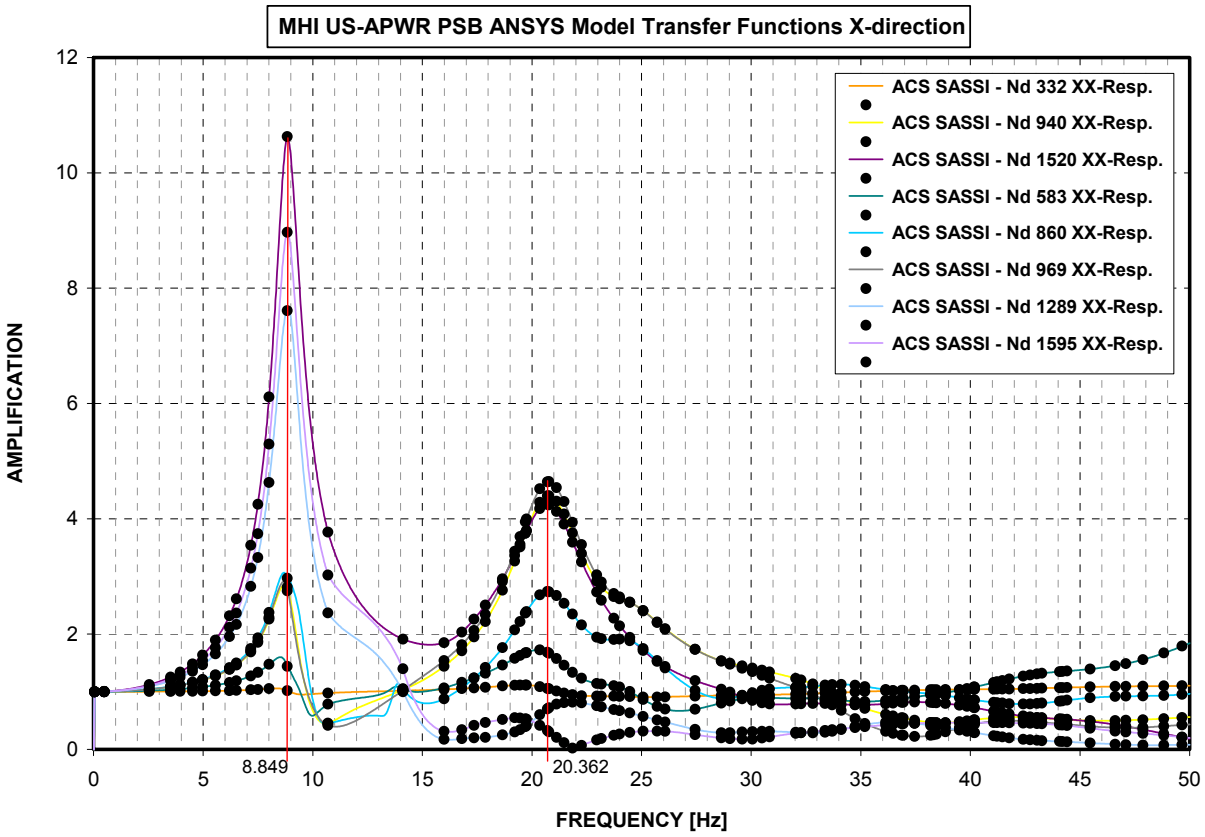

Figure 5.4.2-7 ANSYS Dynamic Model Transfer Functions, X-Direction

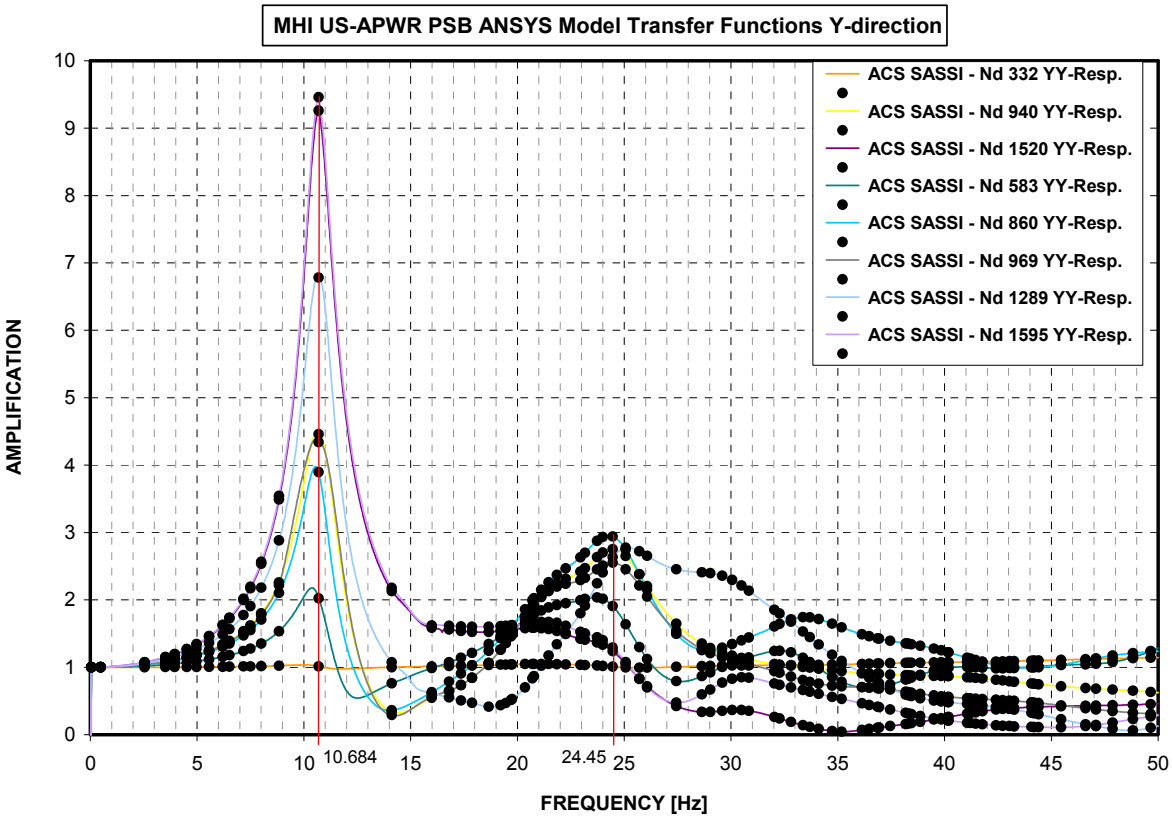

Figure 5.4.2-8 ANSYS Dynamic Model Transfer Functions, Y-Direction

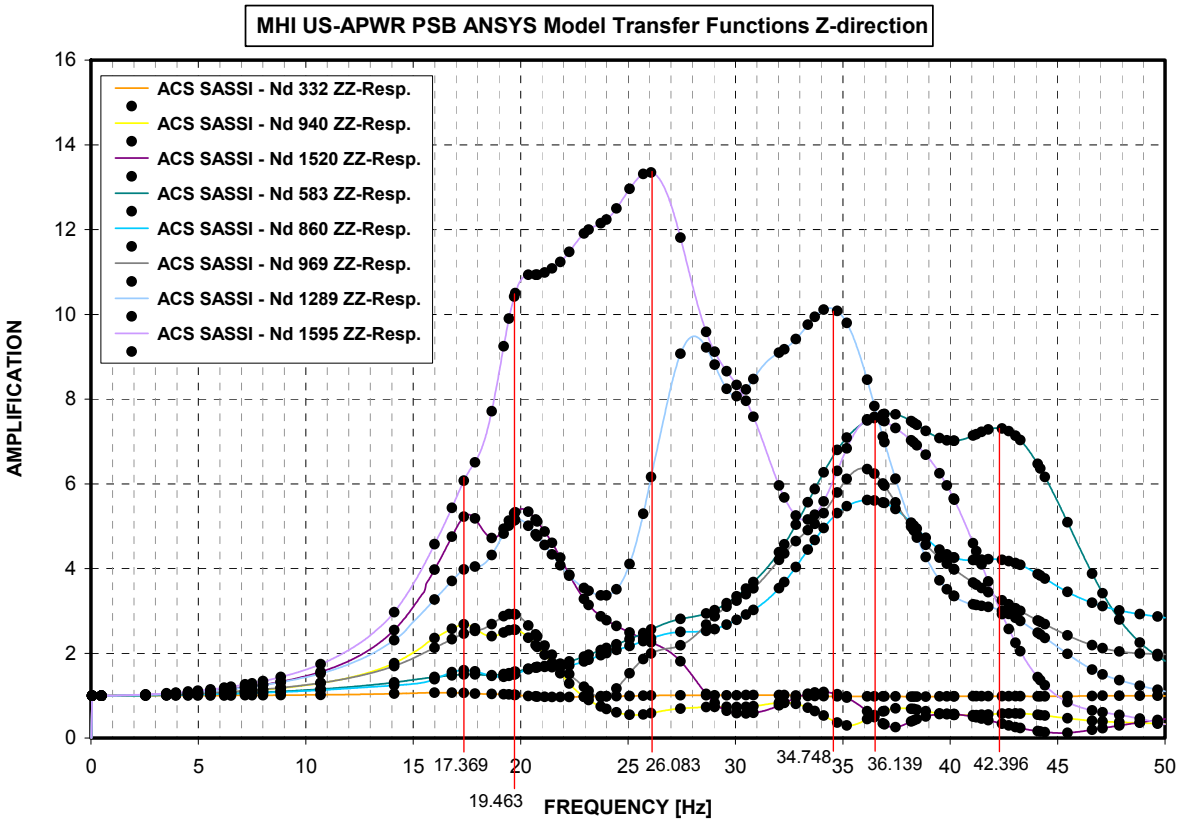

Figure 5.4.2-9 ANSYS Dynamic Model Transfer Functions, Z-Direction

Figures 5.4.2-10 thru 5.4.2-18 show the ARSs at selected representative nodes both from modal-superposition transient dynamic analysis on the detailed static model and SSI analysis on translated ANSYS model. In both analyses, constant mode/material damping ratio of 0.07 is applied.

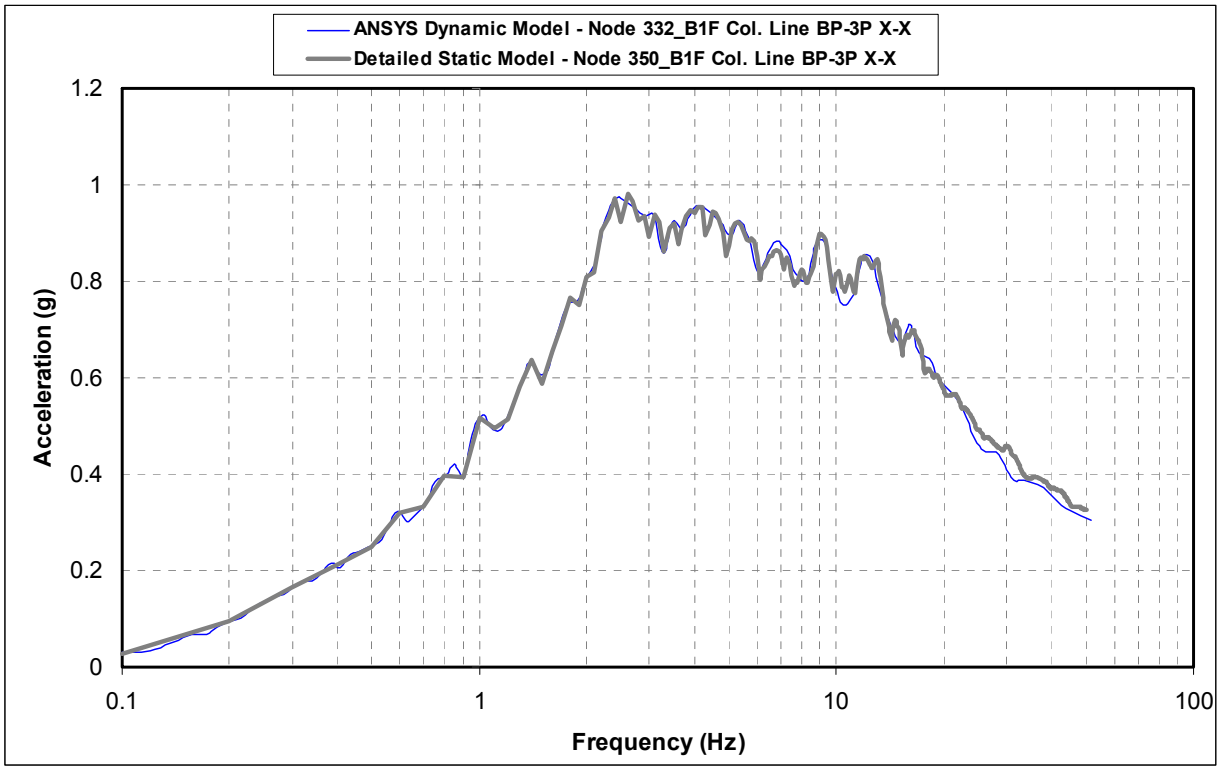

Figure 5.4.2-10 Comparison of ISRS, Basemat X-Direction

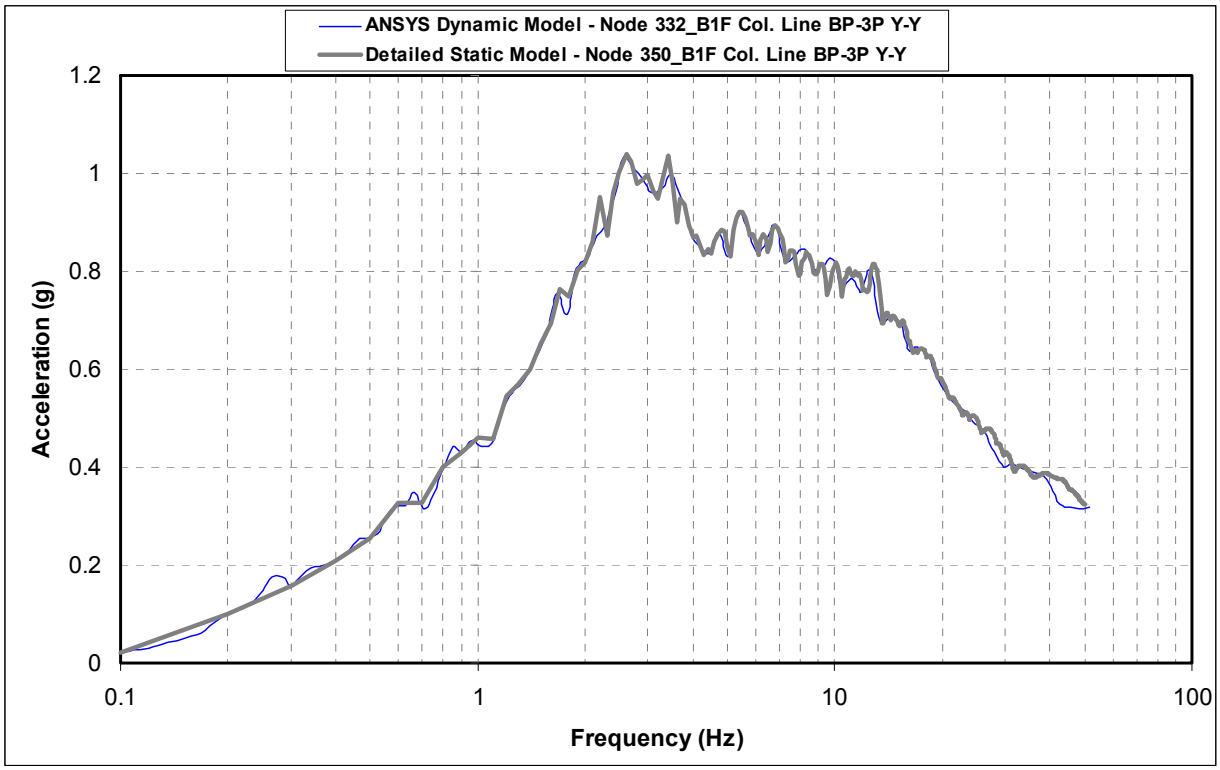

Figure 5.4.2-11 Comparison of ISRS, Basemat Y-Direction

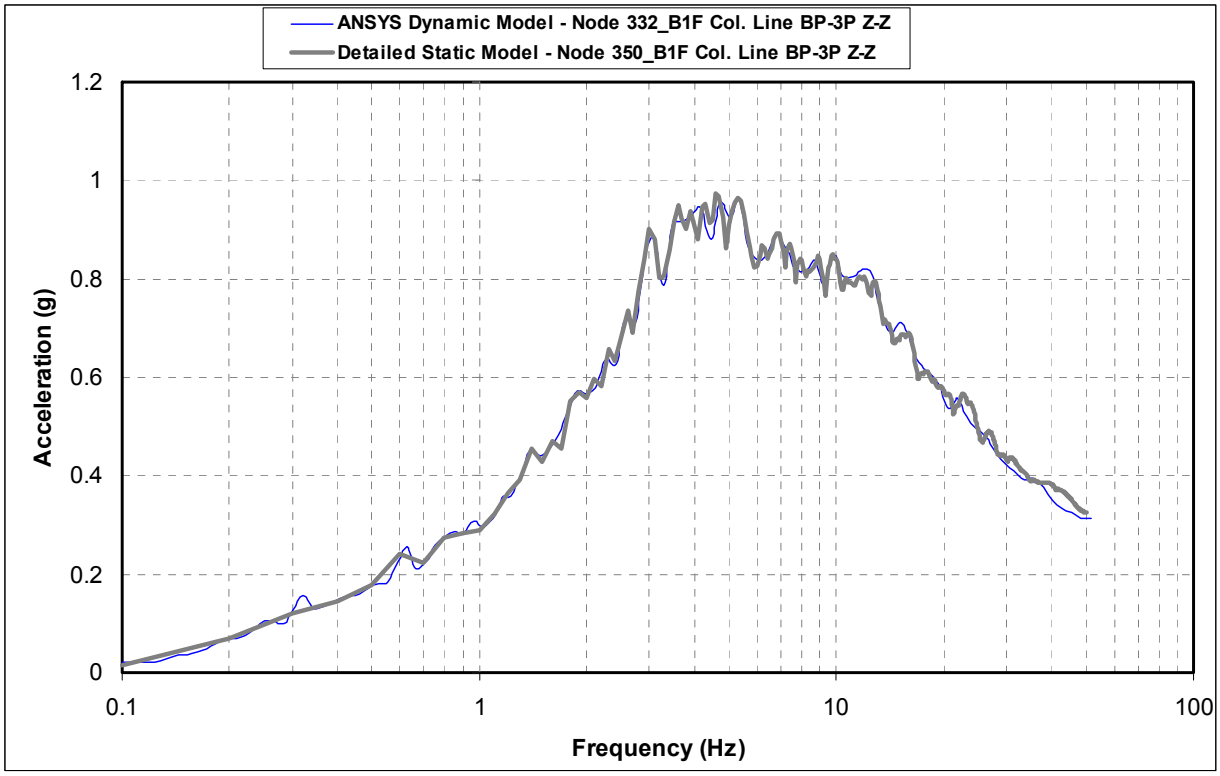

Figure 5.4.2-12 Comparison of ISRS, Basemat Z-Direction

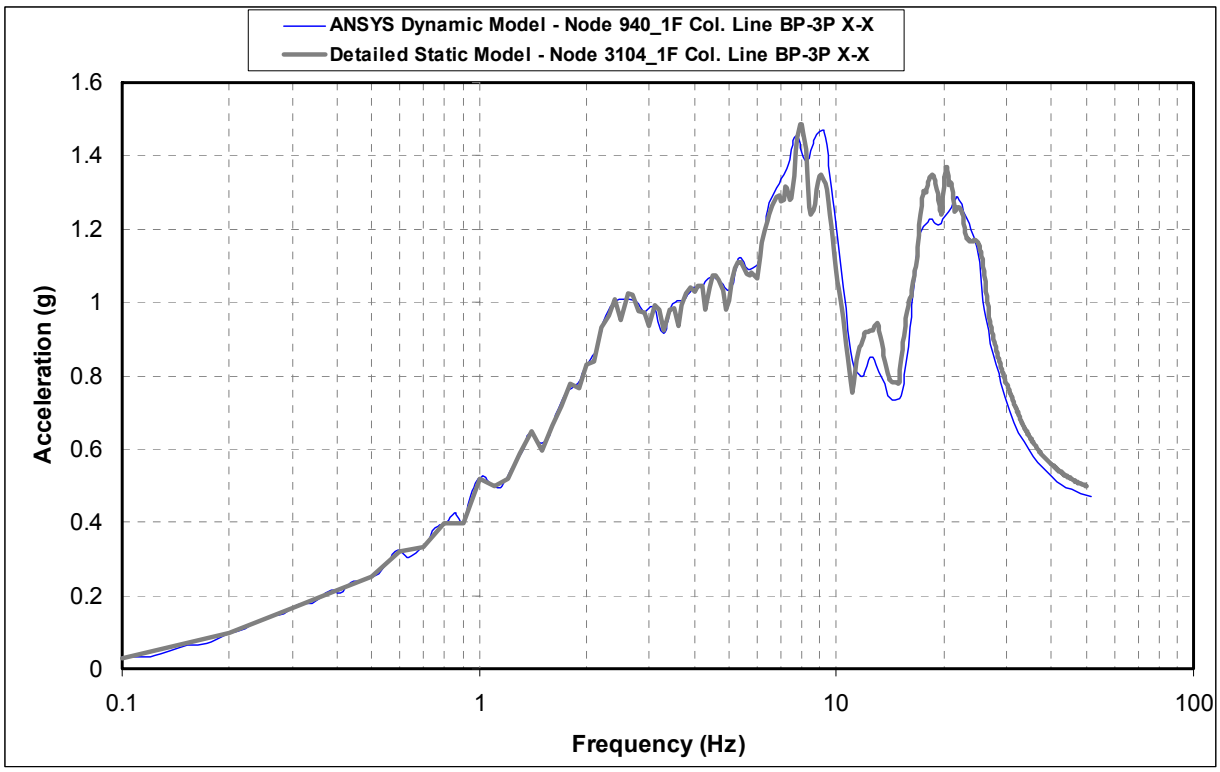

Figure 5.4.2-13 Comparison of ISRS, Ground Floor X-Direction

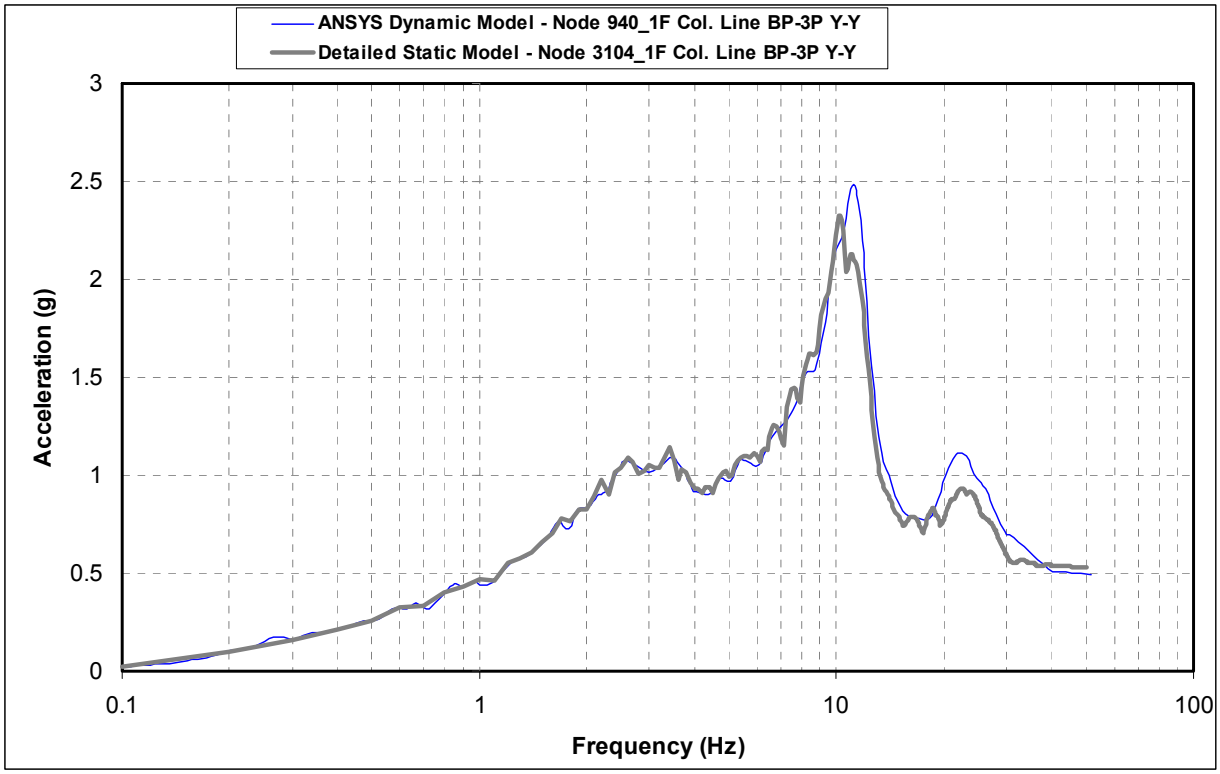

Figure 5.4.2-14 Comparison of ISRS, Ground Floor Y-Direction

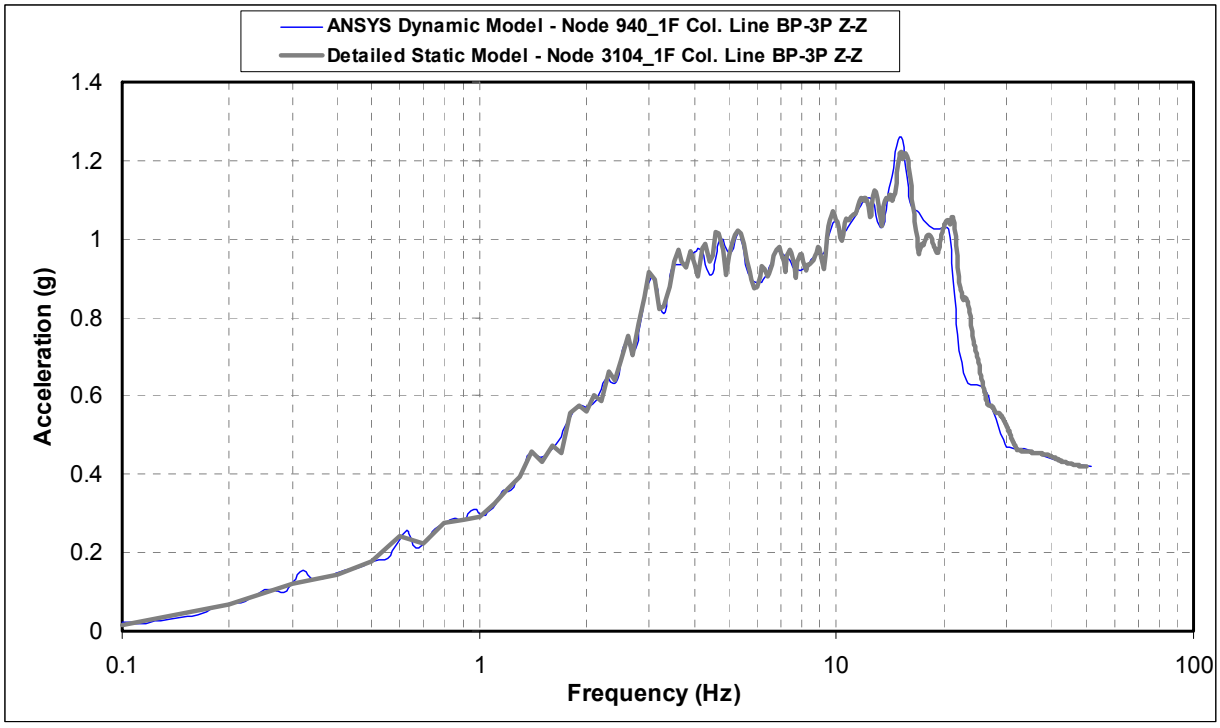

Figure 5.4.2-15 Comparison of ISRS, Ground Floor Z-Direction

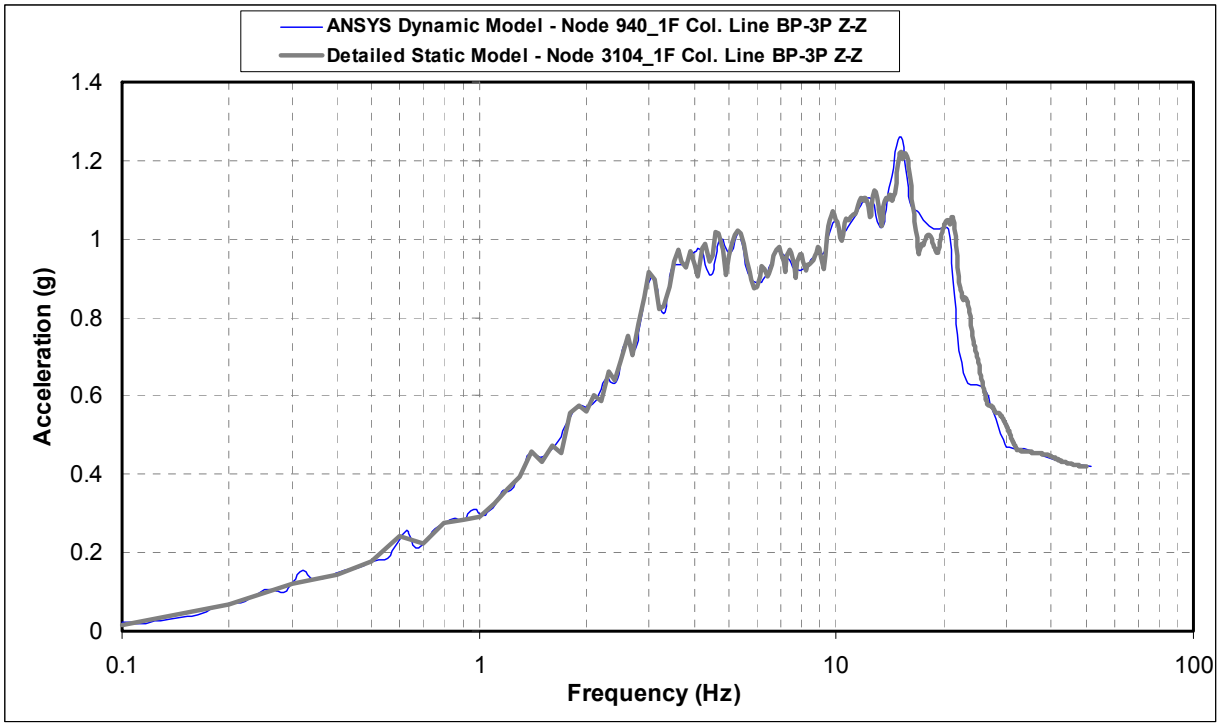

Figure 5.4.2-16 Comparison of ISRS, Roof X-Direction

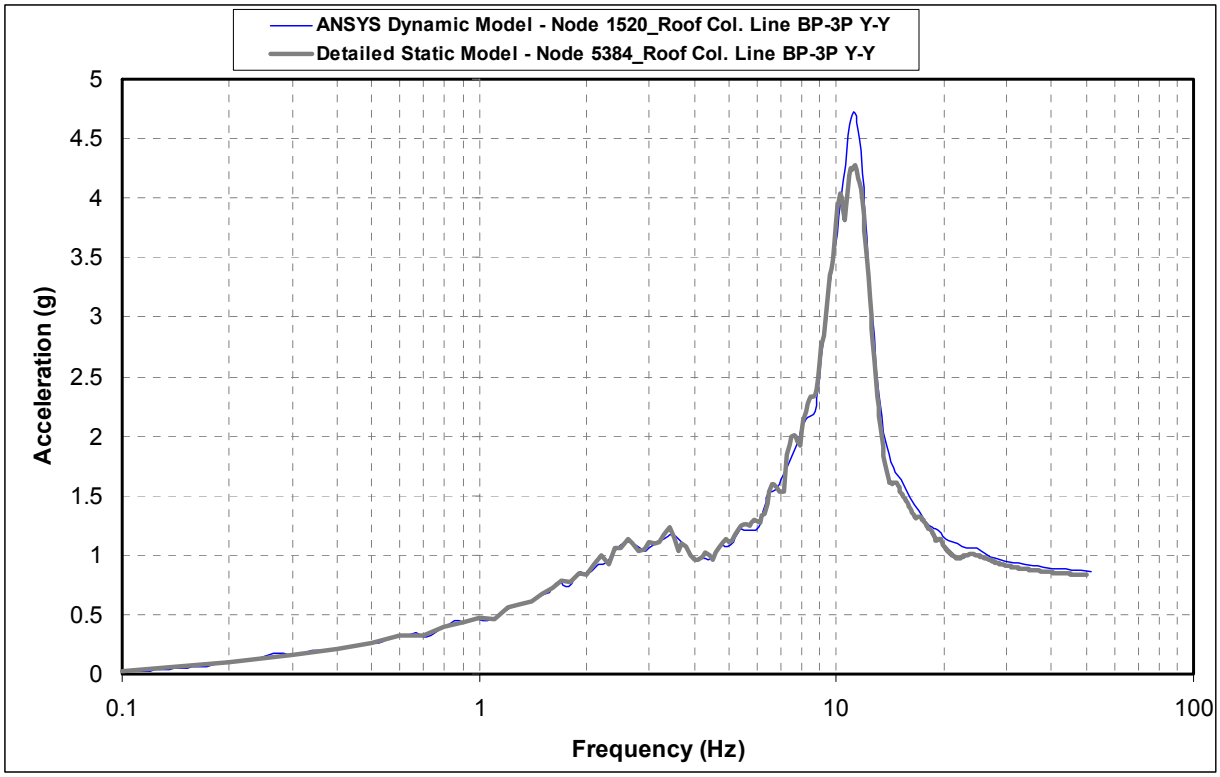

Figure 5.4.2-17 Comparison of ISRS, Roof Y-Direction

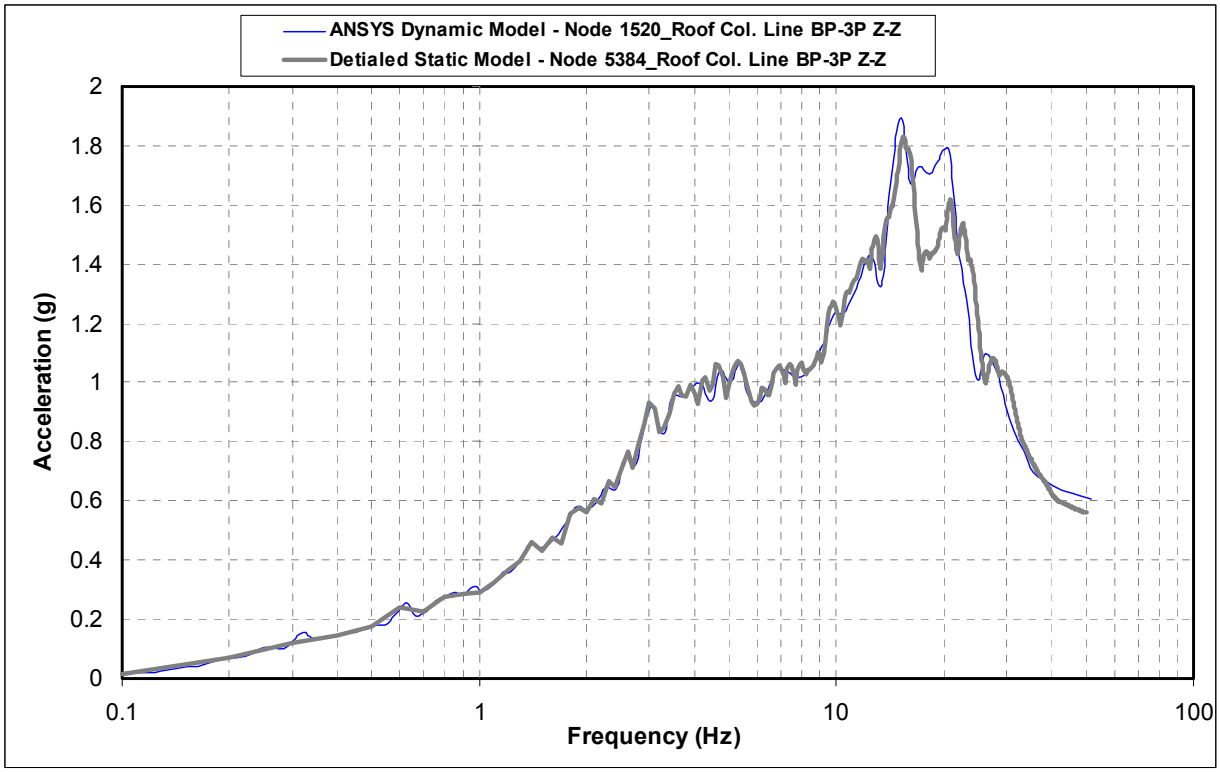

Figure 5.4.2-18 Comparison of ISRS, Roof Z-Direction

5.5 Consideration of Concrete Cracking in Dynamic Analyses

5.5.1 Concrete Cracking of PS/B

Following the procedure/methodology described in Section 4.5, evaluation of the concrete member stress level and stiffness is performed for concrete structural members/shear walls of the PS/B. The calculated stresses along with the concrete capacity of members are tabulates in Tables 5.5.1-1 through 5.5.1-3.

Table 5.5.1-1 shows that the stresses in walls due to in-plane shear are less than the shear capacity. Therefore, in the PS/B FE Dynamic model, elastic in-plane stiffness of the concrete gross section is assigned to the shear walls, i.e. no cracking properties of the concrete is considered for shear wall in-plane stiffness.

Table 5.5.1-2 shows that out-of-plane bending moments of the exterior walls (walls with a thickness of 32 in and 21 in) are greater than the concrete cracking moments. The out-of-plane stiffness of those walls are adjusted for concrete cracking based on Table 3-1 of ASCE 43-05. The detailed calculation of the effective stiffness of the walls indicates that the effective stiffness of Table 3-1 of ASCE 43-05 is sufficiently accurate and adequate to respond the behavior of the walls under loading. Table 5.5.1-2 also indicates that there is no need to consider cracked concrete properties for interior walls (walls with a thickness of 20 inches and 21 inches). Elastic gross section properties are assigned to the interior walls in the PS/B FE Dynamic model.

Based on the results shown in Table 5.5.1-3, flexural stiffness of the floor/roof slabs and beams in the PS/B FE Dynamic model are adjusted for cracked concrete properties based on Table 3-1 of ASCE 43-05. The shear and axial stiffness of the slabs and beams are kept unchanged. For the floor slab at elevation 3’-7”, the calculation indicates that the moment in the service state is smaller than the cracked concrete moment. However, cracked flexural stiffness is applied to this floor slab as well for conservative consideration. It is expected that a more flexible slab will result in a greater amplification of vertical seismic accelerations.

Table 5.5.1-1 PS/B Shear Wall In-Plane Shear Stress/Stiffness Evaluation

Location	Elevation	NS Shear Area Ax ($x10^5$ in^2)	NS Shear Vx (kip)	NS Shear Stress (psi)	Shear hw /lw	capacity capacity Vc (psi)	EW Shear Area Ay ($x10^5$ in^2)	EW Shear Vy (kip)	EW Shear Stress (psi)
PSB2	39'-6"	0.555x0.8	7,170	162	1.42	196	0.577x0.8	7,450	161
PSB1	3'-7"	0.962x0.8	12,500	162	1.18	227	0.936x0.8	13,100	175
BSTP	26'-4"	0.946x0.8	13,359	176	1.18	227	0.934x0.8	13,959	187
		Ax = 0.8 Ag					Ay =0.8Ag		

Table 5.5.1-2 Stiffness Evaluation due to Out-of-Plane Bending

Wall thickness (in)	Moment Ma (k-ft)	Mcr (k-ft)	Ie (in^4)	0.5 Ig (in^4)	0.5Ig / Ie	Comments
32	8.93	6.75	1575	1365	0.87	crack
21	4.91	2.91	359	386	1.07	crack
20	1.48	2.64				No crack (Ie = Ig)
12	0.3	0.95				No crack (Ie = Ig)
Ie = Effective moment of inertia, Ig = Gross mement of inertia						
Ma: Moment in Service State, Mcr: Cracking Moment						

Table 5.5.1-3 Stiffness Evaluation for Beam, Roof, and Floor Slabs

R.Concrete Member	Element No.	Elevation	Thickness (in)	Moment Ma (k-ft)	Mcr (k-ft)	Ie (in^4)	0.5 Ig (in^4)	Comments
Roof Slab	17179	39'-6"	15	1.64	1.48	227	141	crack
Floor Slab	10302	3'-7"	32	5.52	6.75			No crack
Floor Slab	10434	3'-7"	32	4.46	6.75			No crack (Ie = Ig)
Beam	RG5	3'-7"	40	763.85	607.16	252350	184320	crack

5.5.2 Concrete Cracking of R/B Complex

The same procedure/methodology described in Section 5.5.1 is used for the R/B complex. The calculated stresses along with the concrete capacity of members are tabulates in Tables 5.5.2-1 through 5.5.2-3.

From Table 5.5.2-1, it can be concluded that except for the walls at location FH08, FH07 and FH06, the required shear stress of remaining walls are less than or equal to the shear capacity of concrete. However, it should be noted that in the calculation of shear capacity of concrete, the axial compressive force and steel reinforcement have not been considered. In addition, the thickness of walls at FH08, FH07, and HF06 elevations is increased from 2 feet to 3 feet in NS direction and from 1'-9" to 2 feet in EW direction.

Table 5.5.2-2 shows that out-of-plane bending moments of selected elements at various elevations. Except for in the FH/A, the out-of-plane bending moment in the shear walls is less than the cracking moment capacity of the concrete.

Based on the results shown in Table 5.5.2-3, flexural stiffness of the floor and roof slabs in various areas of the R/B FE dynamic model are adjusted for cracked concrete properties based on Table 3-1 of ASCE 43-05. The shear and axial stiffness of the slabs and beams are kept unchanged.

Table 5.5.2-1 R/B Shear Wall In-Plane Shear Stress/Stiffness Evaluation

Location	Elevation (ft)	NS Shear Area Ax ($10^5 in^2$)	NS Shear Vx kip	NS Shear Stress (psi)	hw/lw	Nominal Vc (psi)	EW Shear Area Ax ($10^5 in^2$)	EW Shear Vx kip	EW Shear Stress (psi)	hw/lw	Nominal Vc (psi)
FH08	154.5	0.543	16,000	368	1.23	276	0.922	8,500	115		
FH07	125.67	0.786	22,500	358	1.23	276	0.922	13,600	184	0.43	404
FH06	101	0.794	25,500	401	1.23	276	0.875	17,300	247	0.43	404
RE41	101	1.19	15,400	162	0.15	450	0.479	9,200	240	0.37	415
RE42	101	0.816	7,800	119			0.533	4,400	103		
RE05	115.5	2.04	17,600	108			1.6	18,600	145	0.07	463
RE04	101	2.13	30,800	181	0.08	462	2.17	40,200	232	0.12	455
RE03	76.417	7.02	95,800	171	0.08	461	7.39	108,100	183	0.13	454
RE02	50.167	7.95	137,600	216	0.08	461	7.79	152,100	244	0.12	455
RE01	25.25	8.09	168,200	260	0.07	463	8.29	184,400	278	0.10	458

Table 5.5.2-2 Stiffness Evaluation due to Out-of-Plane Bending (Sheet 1 of 2)

Element No.	Elevation (ft)	Coordination	Thickness (in)	Mcr (kip-ft/in)	Ma (kip-ft/in)	Mcr / Ma	0.5Ig (in^4)	Ie (in^4)	Comment
RE00									
140335	3.58	CL-J, L, C,	44	12.75	3.44	3.71			uncrack
	3.58	cl-a	40	10.5409	1.14951	9.17			uncrack
	3.58	cl-1, 11	40	10.5409	1.17397	8.98			uncrack
140117	3.58	CL-2, C to J	42	11.62	3.74	3.11			uncrack
	3.58	CL-2,10, E to G	30	5.92927	0.88048	6.73			uncrack
RE01									
161753	25.25	CL-2, C to H1	46	13.94	10.29	1.35			uncrack
	25.25	CL-2, E to G	32	6.74619	1.29345	5.22			uncrack
160237	25.25	CL-1,7,6,5,11	40	10.54	8.28	1.27			uncrack
	25.25	CL-A, J,L,	40	10.5409	1.87551	5.62			uncrack
	25.25	CL-H1	32	6.74619	1.5004	4.50			uncrack
	25.25	CL-C	24	3.79473	1.1253	3.37			uncrack
162222	25.25	CL-A, 4b to 5a	93	56.98	121.35	0.47	33515	15419	crack
RE02									
180256	50.17	CL-1, 2, 10, 11	32	6.75	9.55	0.71	1365	1251	crack
	50.17	CL-5,6,7	40	10.5409	2.00977	5.24			uncrack
182484	50.17	CL-A, 4a to 4b	152	152.2	43.39	3.51			uncrack
	50.17	CL-A, J,k, L	40	10.5409	2.33276	4.52			uncrack
	50.17	CL-C,H2	24	3.79473	1.39966	2.71			uncrack
RE03									
183134	76.42	CL-6a, A to A1	85	47.6	1.05	45.3			uncrack
220363	76.42	CL-2, D2 to E	52	17.81	9.15	1.95			uncrack
220016	76.42	CL-1, D2 to E	28	5.17	7.73	0.67	915	704.2	crack
	76.42	CL-1, 11	28	5.16505	1.63002	3.17			uncrack
	76.42	CL-2, 10	32	6.74619	1.86288	3.62			uncrack
	76.42	CL-2a,5,6,7,9b	40	10.5409	2.3286	4.53			uncrack
	76.42	CL-J,K,L	40	10.5409	2.76914	3.81			uncrack
	76.42	CL-A	24	3.79473	1.66149	2.28			uncrack
RE04, RE41, RE42									
240699	101	CL-11	40	10.54	7.15	1.47			uncrack
		CL-1,2a,5,6,7,9b	40	10.5409	1.00745	10.46			uncrack
		CL-H	21	2.90534	0.56915	5.10			uncrack
		CL-K	40	10.5409	1.0841	9.72			uncrack
240522	101	CL-A,C,	24	3.79	2.15	1.76			uncrack
RE05									
	115.5	CL-5,7	20	2.63523	0.61333	4.30			uncrack
	115.5	CL-6	40	10.5409	1.22667	8.59			uncrack
	115.5	CL-L	21	2.90534	0.693	4.19			uncrack
	116.5	CL-K	40	10.5409	1.32	7.99			uncrack

Table 5.5.2-2 – Stiffness Evaluation due to Out-of-Plane Bending
(Sheet 2 of 2)

FH06, FH07,FH08									
	101	CL-2b, 11,A to C	36	8.53815	33.1126	0.26			crack
	101	CL-A,C,	24	3.79473	24.0049	0.16			crack
200110	125.67	CL-11,A to A2	36	8.54	6.08	1.40			uncrack
200045	125.67	CL-1, 5a to 6	24	3.79	3.4	1.11			uncrack
200051	125.67	CL-A, 6 to 6a	24	3.79	5.74	0.66	576	397.9	crack
240944	125.67	CL-C,6 to 6a	24	3.79	4.78	0.79	576	737.9	crack
200390	154.5	CL-C,5a to 6	24	3.79	2.33	1.63			uncrack

Table 5.5.2-3 Stiffness Evaluation for Slabs

Element No.	Elevation (ft)	Coordination	Thickness (in)	Mcr (kip-ft)	Ma (kip-ft)	Mcr / Ma	0.5Ig (in^4)	Ie (in^4)	Comment
200599	154.5	CL-B to C, 5a to 4b	15	17.76	17.04	1.042			uncrack
231572	115.5	CL-J to K, 7 to 6	40	126.492	213.348	0.593	2667	1569	crack
210318	101	CL-E to F, 11 to 10	15	17.76	29.52	0.602	140.63	137.27	crack
	101	CL-D to D2, 2 to 4b	44	153.054	38.593	4.0			uncrack
	101	CL-C to D, 2b to 4b	36	102.458	53.739	1.9			uncrack
183716	76.42	CL-B to C, 6a to 7a	28	61.98	22.056	2.810			uncrack
	76.42	CL-K to L, 7 to 9b	52	213.77	291.828	0.7			crack
	76.42	CL-H to J, 6 to 7	32	80.954	9.255	8.7			uncrack
	76.42	CL-C to D, 2 to 4	30	71.151	38.1743	1.9			uncrack
181639	65	CL-K to L, 7 to 6	40	124.8	102.48	1.22			uncrack
163433	50.17	CL-J to K, 7 to 6	40	126.48	93	1.36			uncrack
	50.17	CL-G to G2, 9a to 10	46	167.284	15.939	10.5			uncrack
	50.17	CL-H to H1, 2 to 3	24	45.537	26.912	1.7			uncrack
142831	25.25	CL-J to K, 7 to 6	40	126.48	173.76	0.7	2666.67	2847.53	crack

6.0 REFERENCES

1. Seismic Design Parameters, NUREG-0800 Section 3.7.1, Revision 3, U.S. Nuclear Regulatory Commission, Washington, DC, March 2007.

2. ACS SASSI, NQA Copy 5 WGI, WGI PO 136-4359, Version 2.2, Ghiocel Predictive Technologies, Inc., 7/23/2007.

3. Dynamic Analysis of the Coupled RCL-R/B-PCCV-CIS Lumped Mass Stick Model, MUAP-08005, Revision 0, Mitsubishi Heavy Industries, Ltd., April 2008.

4. Seismic System Analysis, NUREG-0800 Section 3.7.2, Revision 3, U.S. Nuclear Regulatory Commission, Washington, DC, March 2007.

5. Non-Stationary Spectral Matching, Seismological Research Letters #63, Page 30, Abrahamson, N. A., 1992.

6. Generation of Synthetic Time Histories Compatible with Multi-Damping Design Response Spectra, 9th SMiRT, pages 105-110, Lilhan, K, and W.S. Tseng, 1987.

7. Surface Geology Based Strong Motion Amplification Factors for the San Francisco Bay and Los Angeles Areas, A PEARL report to PG&E/CEC/Caltrans, Award No. SA2120-59652. Silva, W. J.S. Li, B. Darragh, and N. Gregor, 1999.

8. Guidelines for Determining Design Basis Ground Motions, Volumes 1-5, TR-102293, Electric Power Research Institute, Palo Alto, CA, 1993.

   Vol.1: Methodology and Guidelines for Estimating Earthquake Ground Motion in Eastern North America

   Vol. 2: Appendices for Ground Motion Estimation

   Vol. 3: Appendices for Field Investigations

   Vol. 4: Appendices for Laboratory Investigations

   Vol. 5: Quantification of Seismic Source Effects

9. CEUS Ground Motion Project, Final Report, Technical Report TR-1009684, Electric Power Research Institute, Palo Alto, CA, 2004.

10. Technical Basis for Revision of Regulatory Guidance on Design Ground Motions: Hazard- and Risk-Consistent Ground Motions Spectra Guidelines, NUREG/CR-6728, Prepared for Division of Engineering Technology, Washington, DC., 2001.

11. Characteristics of Vertical Strong Ground Motions for Applications to Engineering Design, NCEER-97-0010, Proceedings of the FHWA/NCEER Workshop on the National Representation of Seismic Ground Motion for New and Existing Highway Facilities, I.M. Friedland, M.S Power and R. L. Mayes eds., Silva, W.J., 1997.

12. ANSYS, Advanced Analysis Techniques Guide, Release 11.0, ANSYS, Inc., 2007.

13. Seismic Analysis of Safety-Related Nuclear Structures and Commentary, ASCE 4-98, American Society of Civil Engineers, 1998.

14. Seismic Design Criteria for Structures, Systems, and Components in Nuclear Facilities,

ASCE/SEI 43-05, American Society of Civil Engineers, 2005.

15. Code Requirements for Nuclear Safety Related Concrete Structures, ACI 349-01, American Concrete Institute, 2001.

16. Design Response Spectra for Seismic Design of Nuclear Power Plants, RG 1.60, Revision 1, U. S. Nuclear Regulatory Commission, December 1973.

17. Technical Basis for Revision of Regulatory Guidance on Design Ground Motions: Development of Hazard- and Risk-Consistent Seismic Spectra for Two Sites, NUREG/CR-6769, U.S. Nuclear Regulatory Commission, Office of Nuclear Regulatory Research, Washington, DC 20555-0001, 2002.

18. Empirical Response Spectral Attenuation Relations for Shallow Crustal Earthquakes, Seismological Research Letter, 68(1), pages 94-127, Abrahamson, N.A. and Silva, W.J., 1997.

19. Properties of vertical ground motions, Bulletin of the Seismological Society of America, 92(2), pages 3152-3164, Beresnev, I.A, Nightengale, A.M. Silva, W.J., 2002.

20. Updated Near-Source Ground-Motion (Attenuation) Relations for the Horizontal and Vertical Components of Peak Ground Acceleration and Acceleration Response Spectra, Bulletin of the Seismic Society of America, 93(1), pages 314-331, Campbell, K. W. and Y. Bozorgnia, 2003.